PSEUDO DYNAMIC TESTS OF A FULL-SCALE CFT/BRB COMPOSITE FRAME: DISPLACEMENT BASED SEISMIC DESING AND RESPONSE EVALUATIONS

K.C. TSAI[1], Yuan-Tao WENG[2], Min-Lang LIN[3], Chui-Hsin CHEN[4] Juin-Wei LAI[4] and Po-Chien HSIAO[5]

SUMMARY

AT time of this writing, a full scale 3-story 3-bay concrete filled steel tube (CFT) composite braced frame has been constructed in NCREE with buckling restrained braces (BRBs) and scheduled to be tested in October 2003. The full scale CFT/BRB frame test is part of an international collaboration between researchers in Taiwan and the United States. Measuring 12 meters tall and 21 meters long, the frame is among the largest frame tests of its type ever conducted. The frame is to be tested using the pseudo-dynamic test procedures applying input ground motions from the 1999 Chi-Chi and 1989 Loma Prieta earthquakes, scaled to represent 50%, 10%, and 2% in 50 years seismic hazard levels. This paper describes the displacement-based seismic design procedures adopted in the design of the structural members. A target story drift limit of 0.025 radian for the 2% in 50 years hazard level governs the design strength of the frame. Nonlinear analyses illustrate that the response of individual BRB member can be satisfactorily simulated by using truss elements implemented in two different general purpose nonlinear response analysis programs. Nonlinear dynamic analyses suggest that the peak story drift is likely to reach 0.025 radian after applying the 2/50 design earthquake on the frame specimen. Analytical results also suggest that the arrangement of 4, 3 and 3 actuators, each having 980 kN force capacity, might be necessary for the 1st, 2nd and 3rd floor, respectively. The BRBs at the upper two floors are more vulnerable than those in the first floor. The failure of moment connections is not likely to occur after the applying four earthquake load effects. CFT columns hinging at the base are expected, but should not fail as the rotational demand is moderate.

Keywords: *concrete filled tube, buckling restrained brace, pseudo-dynamic tests, displacement based seismic design, nonlinear analysis*

INTRODUCTION

Through international collaboration between researchers in Taiwan and the United States, a full-scale 3-story 3-bay RC column and steel beam RCS composite moment frame has been tested in October of 2002 in the structural laboratory of National Center for Research on Earthquake Engineering (NCREE) in Taiwan in October 2002 (Chen et al. 2003). In the year 2003, a full-scale 3-story 3-bay CFT column with the buckling restrained braced composite frame (CFT/BRBF) specimen has been constructed and scheduled to be tested in October in a similar manner. The 3-story prototype structure is designed for a highly seismic location either in Taiwan or United States. The typical bay width of 7m and typical story height of 4m have been found common in Taiwan and US building configuration, it also corresponds well with the 1m spacing of the tie down holes on the strong floor and reaction wall of the lab. The total height of the frame, including the grade beam, is within the strong wall height 15m. The 2150mm wide concrete slab is adopted to develop the composite action of the beams. Measuring 12 meters tall and 21 meters long, the specimen is among the largest frame tests of its type ever conducted. The frame will be tested using the pseudo-dynamic test procedures applying input ground motions

[1] *Professor, Department of Civil Engineering, National Taiwan University, Taiwan, e-mail: kctsai@ce.ntu.edu.tw*
[2] *Post-Doctoral Researcher, Department of Civil Engineering, National Taiwan University, Taiwan, e-mail: d88521003@ntu.edu.tw*
[3] *Associate Research Fellow, National Center for Research on Earthquake Engineering, Taiwan, e-mail: mllin@ncree.gov.tw*
[4] *Assistant Research Fellow, National Center for Research on Earthquake Engineering, Taiwan, e-mail: chchen@ncree.gov.tw*
[5] *Graduate Research Assistant, Department of Civil Engineering, National Taiwan University, e-mail: r91521221@ntu.edu.tw*

from the 1999 Chi-Chi and 1989 Loma Prieta earthquakes, scaled to represent 50%, 10%, and 2% in 50 years seismic hazard levels. Following the pseudo-dynamic tests, if no brace is fractured, quasi-static loads will be applied to cyclically push the frame to large inter-story drifts up to the failure of the braces, which will provide valuable data to validate possible failure mechanism and analytical models for large deformation response. Being the largest and most realistic composite CFT/BRB frame ever tested in a laboratory, the test provides a unique data set to verify both computer simulation models and seismic performance of CFT/BRB frames. This experiment also provides great opportunities to explore international collaboration and data archiving envisioned for the Networked Earthquake Engineering Simulation (NEES) initiatives or the Internet-based Simulations for Earthquake Engineering (ISEE) (Yang et al. 2003) launched recently in USA and Taiwan, respectively. This paper focuses on the displacement-based seismic design procedures adopted in the design of CFT/BRB frame specimen. During the planning stage, extensive nonlinear dynamic analyses were also carried out in order to ensure the possible seismic demands would not exceed the force and displacement limits of the test facility. This paper describes the analytical models and evaluates the seismic performance observed from the simulation results. Inelastic static and dynamic time history analyses have been conducted using PISA2D (Tsai and Chang 2001) and OpenSees (Open System for Earthquake Engineering Simulation), developed at National Taiwan University and Pacific Earthquake Engineering Research Center (PEER), respectively.

BASIC DESIGN INFORMATION OF CFT/BRB FRAME SPECIMEN

The large-scale, 3-story CFT/BRB frame shown in Fig. 1 is employed in this experimental research. The prototype three-story building consists of 6-bay by 4-bay in plane. The seismic force in the transverse direction is to be resisted by two CFT/BRB frames symmetrically positioned in the building as shown in Fig. 1. Prior to the frame test, a series of subassembly tests have been completed in the structural laboratory in NCREE and some recommendations have been concluded for the design of the connections. As shown in Fig. 1, the height of the CFT/BRB frame specimen measured from the top of the foundation is 12 m. Other design and analytical parameters include:

1. Loading
   (1) Dead Load: for the 1st and 2nd floor, it is 3.68 kN/m^2; for the 3rd floor, it is 3.24 kN/m^2
   (2) Live Load: for all floors, it is 2.45 kN/m^2
2. Design Codes
   a. Taiwan seismic building code draft (2002, denoted as "Taiwan code 2002")
   b. All steel beams and CFT columns are designed by using AISC-LRFD
   c. All P-M curves of the CFT columns for nonlinear frame response analysis are constructed using EC4 (CEN, 1992)
3. Design Load Combinations
   a. 1.2 DL + 0.5 LL + 1.0 EQ
   b. 0.9 DL + 1.0 EQ
   c. 1.2 DL + 1.6 LL
4. Story Seismic Mass: for the 1st and 2nd floors: 31.83 ton; 3rd floor: 25.03 ton (per CFT/BRB frame)
5. Materials
   a. Steel: All steel is A572 Gr.50, f_{ys}=350 MPa (50 ksi)
   b. Infill Concrete in CFT columns: f_c' =35 MPa (5000 psi)

In the two identical prototype CFT/BRB frames, only the two exterior beam-to-column connections (Fig. 1) in each floor are moment connections, all other beam-to-column connections are assumed not to transfer any bending moment. The details of the moment connections are schematically given in Fig. 2 for the top through the first floor beams.

DISPLACEMENT-BASED SEISMIC DESIGN PROCEDURE

This paper presents the results of applying the displacement-based seismic design (DSD) procedures (Loeding et al 1998; Medhekar and Kennedy 2000), to the design of the 3-story CFT/BRB frame specimen. The multi-mode design procedures adopted for this frame specimen were also studied and can be found in the reference (Weng 2003). In this paper, it is assumed that the earthquake responses of the 3-story 3-bay CFT/BRB frame are essentially the first vibration mode. The DSD details follow:

1. Select acceptable (target) maximum story drift levels

A. Design Earthquake Acceleration Response Spectra

Fig. 3a and Fig. 3b consider Taiwan seismic code draft updated in 2002. It stipulates, for a hard rock site, the

S_a(T=1 sec) values for earthquake hazard of 10% chance of exceedance in 50 years (10/50 Design Earthquake, DE) and 2/50 (Maximum Considered Earthquake, MCE) earthquakes as 0.68g and 0.91g, respectively. These are the same as those used for the RCS frame tests in 2002. The 5% damped S_a values for TCU082EW records adopted in the RCS frame tests are also shown on Figs. 3a and 3b. The corresponding PGA values for the 10/50 and 2/50 levels of excitations are 0.46g and 0.62g, respectively, for the TCU082EW record. Similarly, for the LP89g04NS record, the corresponding PGA values for the 10/50 and 2/50 levels of excitations are 0.40g and 0.54g, respectively.

B. Performance Criteria for the CFT/BRB Frame

Since no performance criteria, prescribed for the CFT/BRB frame system, can be found in the model seismic building design standards, the proposed performance criteria is chosen as indicated in Table 1 for the two hazard levels considered in this study. For the 10/50 and 2/50 events, the inter-story drift limits are set at 0.02 and 0.025 radians, respectively.

2. **Calculate the maximum displacement profile**

It is assumed that structural first modal design displacement profile can be simplified as an inverted triangle. If a target drift level is selected in Step 1, then each story displacement can be decided. For example, under the 10/50 event, the story drift limit is 0.02 radian, thus the target roof displacement is 24cm; for the 2/50 event and the corresponding target drift angle of 0.025 radian, the target roof displacement is 30cm.

3. **Calculate the system displacement**

The system displacement is equal to the effective displacement and given by

$$\delta_{eff} = \sum_{i=1}^{N} m_i \delta_i^2 / \sum_{i=1}^{N} m_i \delta_i \tag{1}$$

where m_i is the story mass, δ_i is the i^{th} target story displacement, N is the story number of the building, then δ_{eff} is the effective displacement. This step essentially translates the actual MDOF structure to the substituted SDOF structure through displacements.

4. **Estimate system ductility from the properties of buckling restrained braces**

The relationship between brace deformation and inter-story drift angle is approximated as given by Eq. 2 and Fig. 4 (Tsai et al. 2002).

$$\varepsilon_{wp} = (\theta \quad sin\, 2\varphi) / 2 \tag{2}$$

$$\varepsilon_c \approx \varepsilon_{wp} / \alpha_c \tag{3}$$

where θ is the story drift angle, φ is the angle between the horizontal beam and the brace showed in Fig.4, and ε_c is the strain of the brace core segment, $\alpha_c = L_c / L_{wp}$ (L_c and L_{wp} are defined in Fig. 5). Eq. 3 is not applicable when the braces remain elastic, but should be a good upper bound estimate of the brace core strain when the braces is undergone significant inelastic deformations. When the braces yield, $\varepsilon_c = \varepsilon_{cy} = f_{sy} / E_S$, the i^{th} story drift $\theta_{yi,BRB}$ corresponds to the brace yielding can be estimated as:

$$\theta_{yi,BRB} = 2 \times \varepsilon_{cy} \times \alpha_c / sin\, 2\varphi \tag{4}$$

Eq. 4 only considers the elastic deformation contribution of BRBs to the total yield story drift. Therefore, the i^{th} yielding story drift θ_{yi}, including the effects of all other member deformations in the same story, is assume to be at least $1.25\theta_{yi,BRB}$. If θ_{mi} is the target drift of the i^{th} story calculated from the target displacement profile, then the story ductility can be computed from:

$$\mu_i = \theta_{mi} / \theta_{yi} \tag{5}$$

After calculating all the story ductilities from Eq. 5, the average of all story ductilities can be taken as the system ductility. If the BRB is made from A572 Gr.50 steel, its minimum yield strain ε_{cy} is about 0.00172. Assume that the core length ratio α_{ci} for braces at i^{th} floor is about 0.5, then the story ductility can be calculated by Eqs. 2 through 5, and the results show in Table 3a that the averaged system ductility demands for the 10/50 and 2/50 events are 9.19 and 11.5, respectively. The actual material test results given in Table 2 can be used to refine the estimations of the ductility demand. Given the actual steel core strength and the length ratio α_{ci} for braces at 1^{st}, 2^{nd} *and* 3^{rd} floor as 0.60, 0.49 and 0.57, respectively, then the story ductility and the averaged system ductility demands (shown in Table 3b) for the 10/50 and 2/50 events are 7.28 and 9.10, respectively.

5. **Compute the effective structural vibration period**

Applying the R_y μ T relationships suggested by Newmark and Hall (1982):

$$S_{d,in} = \frac{\mu}{R_y}\left(\frac{T}{2\pi}\right)^2 S_a = \frac{\mu}{R_y} S_d \tag{6}$$

Eq. 6 provides a convenient way to determine the deformation of the inelastic system from the elastic design spectrum, where $S_{d,in}$ is the inelastic peak deformation of the SDOF system, S_a and S_d are the elastic design spectral acceleration and displacement, respectively, R_y is the yield strength reduction factor. For the smoothened design response spectra given in Fig. 4 for a hard site, it is stipulated in the latest Taiwan seismic force design standards that:

$$R_y = \begin{cases} \mu & ; \quad T \geq T_0 \\ \sqrt{2\mu - 1} + \left(\mu - \sqrt{2\mu - 1}\right) \times \dfrac{T - 0.6T_0}{0.4T_0} & ; \quad 0.6T_0 \leq T \leq T_0 \\ \sqrt{2\mu - 1} & ; \quad 0.2T_0^D \leq T \leq 0.6T_0 \\ \sqrt{2\mu - 1} + \left(\sqrt{2\mu - 1} - 1\right) \times \dfrac{T - 0.2T_0}{0.2T_0} & ; \quad T \leq 0.2T_0 \end{cases} \tag{7}$$

$$T_0^D = S_{D1} / S_{DS} \quad ; \quad T_0^M = S_{m1} / S_{MS} \tag{8}$$

where corner period is $T_0 = T_0^D\left(for\ 10/50\right)\ or\ T_0^M\left(for\ 2/50\right)$. It should be noted that for the 10/50 event (Fig. 3a), $S_{DS} = 1.18$ g and S_{D1}=0.68g, while for the 2/50 event (Fig. 3b), S_{MS}=1.46g and S_{M1}=0.91g. Using Eqs. 6 through 8 and applying the system ductility demands 7.28 and 9.10, inelastic displacement response spectra $S_{d,in}$ can be constructed as shown in Fig. 6 from the response spectra given in Figs. 3a and 3b for the two noted earthquake hazards. Applying the target displacement profile for the 10/50 event using Eq. 1, the effective displacement δ_{eff} is 0.18 m. Similarly, for the 2/50 event, the effective displacement is 0.23 m. Intersecting the effective target displacements of 0.18 m and 0.23 m on the inelastic displacement response spectra shown in Fig. 6, the effective first vibration period $(T_{eff})_1$ during the 10/50 and 2/50 events can be found as 1.42 and 1.32 second, respectively. Noted that for the 10/50 design hazard against a roof drift limit of 0.02 radian, the system appears to be less demanding in terms of strength and stiffness, thus have resulted in a lighter design, than that for the 2/50-0.025 hazard/performance criteria. This could help in explaining why the $(T_{eff})_1$ values for two different designs, during the 10/50 and 2/50 events, are found as 1.42 and 1.32, second, respectively. In Fig. 6, the elastic displacement response spectra (μ=1.0) are also given.

6. **Calculate the effective mass**

The effective mass is calculated by Eqs. 9 and 10:

$$c_i = \delta_i / \delta_{eff} \tag{9}$$

$$m_{eff} = \sum_{i=1}^{N} m_i c_i \tag{10}$$

7. Calculate the effective stiffness K_{eff}:

$$K_{eff} = 4\pi^2 m_{eff} / \left(T_{eff}\right)_1^2 \tag{11}$$

8. **Calculate the design base shear**

The design yield base shear V_d is calculated from Eqs.12 and 13:

$$V_b = K_{eff} \times \delta_{eff} \tag{12}$$

$$V_d = V_b / \left[1 + \alpha_h\left(\mu - 1\right)\right] \tag{13}$$

where α_h is the bilinear stiffness ratio, generally α_h can be taken as 0.1. The design base shears, 1575 and 2021 kN represent the stage of significant system yielding for the two events. It is evident that the 2/50-0.025 hazard/performance criteria govern the design. For the purposes of research, separate studies also investigated the seismic demands imposed on different frames designed for both the 10/50 and 2/50 hazard levels considering various design story force computation strategies (Weng 2003).

9. **Distribute the design base shear over the frame height**

The design base shear is distributed over the frame height using Eq. 14 to get the lateral design story forces.

$$F_i = m_i \delta_i V_d / \sum_{i=1}^{N} m_i \delta_i \tag{14}$$

Since the system ductility affects design base shear as shown in Eq. 13, the triangular story force distributions

are listed in Table 4 for four different designs considering the two hazard levels (10/50 and 2/50) and the two material strengths (nominal A572 GR50 versus the tensile coupon strengths). Frames 10/50-Tri and 2/50-Tri consider the brace nominal strength and triangular force distribution for the 10/50 and 2/50 events, respectively. Frames 10/50-TriMR and 2/50-TriMR denotes the designs using the actual material strength. The 28-day 5000 psi (35 MPa) concrete nominal compressive strength for CFT columns is considered in all the frame designs. The cylinder test results will be adopted in future analysis. However, the effects of its variations are believed less significant at this stage as most of the story shears should be resisted by steel BRBs. Table 4 also gives the four different frame fundamental periods results from the variation of the designed cross-sectional area along the length of the brace. Details will be further discussed below.

10. **Conduct structural analysis and design the members for the CFT/BRB frame**

Assume 80% of the total horizontal shear at each story is resisted by two BRBs, therefore, the preliminary selection of the core cross sectional area A_c of BRBs can be determined from the following:

$$A_c = P_{brace} / F_y \tag{15}$$

Since the BRBs are the primary energy dissipation element under the two levels of earthquake, the connecting beams and the column members need to be designed considering the capacity design requirements. Fig. 7 gives typical force versus deformation responses with respect to the actual yield capacity ($A_c \times F_{y,actual}$) for BRB specimens tested in National Taiwan University using A572 Gr.50 steel (Tsai and Lin 2003). It is evident that under large cyclic increasing strains, the peak compressive force responses are slightly larger than tensile force responses. In addition, the strain hardening effects factor of Grade 50 steel is about 1.25 (for typical A36 steel, strain hardening factor can reach 1.5). Therefore, the maximum possible brace force can be estimate as follows:

$$P_{max} = \beta \times \Omega \times \Omega_h \times P_y \tag{16}$$

where P_y is the nominal tensile yield strength, Ω accounts for possible material overstrength, Ω_h represents the effects of strain hardening, and β (of about 1.1) considers the ratio between the peak compressive and tensile forces. Since the actual yield strength obtained from the tensile coupon tests will be employed to adjust the final BRB cross sectional area before fabrication, the material overstrength factor is eliminated in the capacity design of members or connections for the CFT/BRB frame specimen. The beams given in Table 5 satisfy the capacity design principle. It considers the horizontal brace force components as beam axial loads and the flexural demand resulted from a vertical unbalanced concentrated force of $0.1\Omega_h P_y \sin\varphi$ acting upward at the center of the beam span as depicted in the free body diagram Fig. 8. The LRFD specifications apply:

$$P_u/(\varphi_c P_n) \geq 0.2 \ : \qquad P_u/(\phi_c P_n) + \frac{8}{9} M_u / \left[\left(1 - \frac{P}{P_e} \right) \phi_b M_n \right] \leq 1.0 \tag{17}$$

where $P_n = F_{cr} A_g$, $P_e = \dfrac{\pi^2 EI}{(kl)^2}$, $\varphi_c = 0.75$ (tension) or 0.85 (compression), $\phi_b = 0.9$

Note that the bottom beam flange is not laterally braced except by transverse beams at the center point of span. Accordingly, P_n and M_n in Eq. 17 are conservatively computed (without considering the effects of the concrete slab) from an unbraced length of 3.5 m for the capacity design of left beam segment shown in Fig. 8. The selection of the two interior columns is concrete filled 400 mm diameter steel pipe with a wall thickness of 9 mm, while the two exterior CFT columns are 350 mm square 9 mm thick. The 28 days compressive strength of concrete is 5000 psi (35 MPa). The beams in the two end bays in each floor are chosen the same as the interior bay. In order to simplify the construction and the behavior of the specimen, only the exterior beam ends are moment connected to the exterior column. At all beam-to-column moment connecting joints, the strong column weak beam and strong panel zone weak beam criteria are satisfied. It meets the requirements of simultaneously applying a strain hardening factor of 1.1 and a factor of 1.25 to account for the concrete slab effects on the bare steel beam nominal flexural capacity. This demand is checked against the column or panel zone strength without adopting the strength reduction factor. An elastic model was then constructed using the SAP2000N (CSI Inc., 1997) program to check the distributions of the story shear in the braces and columns. The elastic axial stiffness computation of the CFT columns follows the LRFD specifications. The effects of flexural stiffness of the CFT columns have been investigated by considering the full composite or bare steel section. After very few iteration, it is found in the elastic model that the final selection of the braces and other member for Frame 2/50-TriMR shown in Table 5 satisfy all the requirement noted above. In particular, the BRBs in each story will reach yielding at the proximity of the design story shear. The total core cross sectional area for each individual brace is 15, 25 and 30 cm^2 for the 3rd, 2nd and 1st story, respectively. The fundamental vibration period of the four design results noted above ranges from 0.68 to 0.72 second. In addition, the effects of varying the flexural stiffness of the CFT columns from fully composite (using LRFD specification) to the bare steel have been found insignificant, only change the fundamental vibration period from 0.68 to 0.71 second. Consequently, an averaged CFT flexural stiffness (resulting in a fundamental period of 0.70 second) has been adopted in all the analysis

presented herein.

Three different types of moment connections, namely through beam, external diaphragm and bolted end plate types, varying from the first floor to the third floor are chosen and fabricated for the exterior beam-to-column connections (Fig. 2). Three types of BRBs, including the single-core, double-cored and the all-metal BRBs, have been installed in the three different floors. In particular, two single-cored unbonded braces (UBs), each consisting of a steel flat plate in the core, were denoted by Nippon Steel Company and have been installed in the second floor. Each UB end to gusset connection uses 8 splice plates and 16-24mmϕ F10T bolts. The two BRBs installed in the third floor are double-cored constructed using cement motar infilled in two rectangular tubes (Tsai et al. 2003) while the BRBs in the first floor are also double-cored but fabricated with all-metal detachable features (Tsai and Lin 2003). Each end of the double-cored BRB is connected to a gusset plate using 6- and 10-22mmϕ F10T bolts at the third and first floor, respectively.

ANALYTICAL MODELS

In this section, the structural member and properties are based on Frame 2/50-TriMR (Tables 2 and 5) using PISA2D and OpenSees.

PISA2D model
All BRBs were modeled using the two-surface plastic (isotropic and kinematic) strain hardening truss element (Fig. 9). All the CFT and beam members were modeled using the bi-linear beam-column elements (Fig. 10). The P-M curves of the CFT columns are constructed using EC4 (CEN 1992) before multi-linearized as shown in Fig. 11. A leaning column is introduced in the frame model in order to simulate the 2^{nd} order effects developed in the gravity columns.

OpenSees Model
All the CFT columns and steel beams of the frame were modeled using the flexibility-based nonlinear beam-column element with discretized fiber section model as illustrated in Fig. 12. All BRBs were modeled using the truss element with bilinear isotropic strain hardening. A leaning column arrangement has also been adopted in OpenSees model.

Element Responses
Cyclic analyses on basic elements are exercised to verify the differences of the elements adopted in PISA2D and OpenSees. Cyclic axial displacement history given in Fig. 13 was applied to two different truss elements in order to validate the analytical BRB models. Similarly, in order to compare the bi-linear and the fiber CFT beam-column models, cyclic lateral displacement history as shown in Fig. 14 was applied to a cantilever. It is evident that the hysteretic behavior of BRB member simulated either by PISA2D or OpenSees shown at Fig.15 is satisfactory and well agree with the experimental results obtained in a NTU test using A572 Gr.50 BRB (Tsai and Lin 2003). On the other hand, because the bi-linear beam-column element constructed by PISA2D does not effectively consider the strength degrading behavior of the concrete, significant difference on the responses of CFT column member shown in Fig. 16 and Fig. 17 is induced. For this reason, a three-parameter degrading beam-column element implemented in the PISA3D program is being applied in a separate study, and the results will be reported in the future after the frame tests are completed. In addition, since most of the story shear is resisted by the braces, preliminary analyses have confirmed that the effects of the CFT column hysteretic behavior (whether it is bi-linear or degrading) are rather insignificant.

NONLINEAR ANALYSIS AND SEISMIC DEMAND EVALUATIONS

As noted above, two ground accelerations, TCU082EW and LP89g04NS shown in Fig. 18 were adopted in the RCS frame tests in 2002 (Chen et al. 2003). In addition, similar to the earthquake intensities and sequence arranged for RCS frame tests, Fig. 19 shows the arrangement of the earthquake sequence adopted in studying the effects of four continuous earthquake events. These four events are 50/50 (using TCU), 10/50 (using LP), 2/50 (using TCU), another 10/50 (using LP). Fig. 20 and Fig.21 present the roof displacement and lateral story force demands imposed by the four continuous events. Nonlinear static push over analyses conducted for Frame 2/50-TriMR using PISA2D and OpenSees are shown in Fig. 22. Figures. 23 and 24 show the peak story drift and force demands imposed by the four continuous events. The peak story drift distributions shown in Fig. 23 indicate that the target maximum design story drift of 0.025 radian is reached in the first or third floor. The peak lateral story force distributions shown in the Fig. 24 suggest that the first floor may need more actuators than the upper two floors. In addition, four actuators of 980kN force capacity each at the first floor might be required for

the proposed testing of the CFT/BRB frame specimen. The ratios between the cumulative inelastic axial deformation and the tensile yield displacement (Sabelli 2000), taken as the plastic deformations occurring in a brace summed over all cycles throughout the entire response history, in either tension or compression, divided by the tensile yield displacement of the BRB brace member, are listed in Table 6. It reaches 133 and 455 after undergoing the first 10/50 event and the four earthquake events, respectively, at one top floor brace. The cumulative deformations computed from the analyses suggest that the BRBs at the 3rd and 2nd floors are much more vulnerable than those in the first floor. A total of 402 or 455 times the yield deformation (Table 6) is reaching the capacity of a typical BRB tested in NTU (Tsai and Lin 2003). Thus, the fracture of BRBs after applying four strong earthquakes could occur at the upper floors. Fig. 25 illustrates the extents and the distributions of the maximum inelastic deformations developed in the Frame 2/50-TriMR after the four earthquake excitations analyzed by using PISA2D. These analytical results also suggest that the inelastic rotational demands imposed on beam-to-column moment connections are greatly reduced. Failure of moment connections is not likely to occur during the four earthquake excitations.

CONCLUSIONS

Based on these analyses, summary and conclusions are made as follows:

- Since most the story shear is resisted by the BRBs, the significant difference in post-yield strength observed in Fig. 22 is most likely induced by the difference in the constitutive models adopted in PISA2D and OpenSees programs for the truss element.
- The peak story drift is likely to reach 0.025 radian after applying the 2/50 design earthquake on the specimen.
- As for the number of actuators each having 980kN force capacity, analytical results shown in Fig. 24 suggest that the arrangement of 4, 3 and 3 actuators might be necessary for the 1st, 2nd and 3rd floor, respectively.
- The variation of the residual displacements evidenced in Fig. 20 seems to suggest that the hysteretic behavior of the BRBs observed in Fig. 15 could have significant effects on the magnitude of the residual displacement.
- The BRBs at the upper two floors are more vulnerable than those in the first floor. The failure of moment connections is not likely to occur. CFT column hinging at the base is expected, but the rotational demand is moderate.

ACKNOWLEDGEMENTS

The National Science Council of Taiwan provided the financial support for this experimental research program. Nippon Steel Company donated two unbonded braces which have been installed in the 2nd floor of the frame specimen. Valuable suggestions provided by many Taiwan and US professors on this joint effort are gratefully acknowledged.

REFERENCES

AISC(American Institute of Steel Construction), *Seismic Provisions for Structural Steel Buildings*, Chicago, IL, 1997.

CEN, *Design of Composite Steel and Concrete Structures-Part 1-1: General Rules and Rules for Buildings*, EuroCommittee for Standardization, Brussels, Belguim, 1992.

Chen, C.H., Lai, W.C. Cordova, P., Deierlein, G. G. and Tsai, K.C., "Pseudo-Dynamic Test of a Full-Scale RCS Frame: Part 1 – Design, Construction and Testing", Proceedings, International workshop on Steel and Concrete Composite Constructions, Taipei, Oct. 2003.

Loeding, S., Kowalsky, M.J., and Priestley, M.J.N., "Displacement-based Design Methodology Applied to R.C. Building Frames", *Structural Systems Research Report SSRP 98/08*, Structures Division, University of California, San Diego, 1998, 269 pp.

Medhekar, M. S. and Kennedy, D. J. L., "Displacement-Based Seismic Design of Buildings-Theory", *Engineering Structures*, Vol.22, No.3, 2000, 201-209.

Newmark, N. M. and Hall, W. J., "Earthquake Spectra and Design", Earthquake Engineering Research Institute, Berkeley, Calif., 1982, 103 pages.

Sabelli, R., Mahin, S. and Chang, C., "Seismic Demands on Steel Braced Frame Buildings with Buckling-Restrained Braces", *Engineering Structures*, Vol.25, No.2, 2000, 655-666.

Tsai, K.C., and Chang, L.C., "User Manual for the Platform and Visualization of Inelastic Structural Analysis of 2D Systems PISA2D and VISA2D", Center for Earthquake Engineering Research, National Taiwan University, *Report No. CEER/R90-08*, 2001.

Tsai, K.C., Hwang, Y.C., Weng, C.S, Shirai, T, and Nakamura, H., "Experimental Tests of Large Scale Buckling Restrained Braces and Frames", Proceedings, Passive Control Symposium 2002, Tokyo Institute of Technology, Tokyo, December 2002.

Tsai, K.C. and Lin, S.L, "A Study of All Metal and Detachable Buckling Restrained Braces", Center for Earthquake Engineering Research, National Taiwan University, *Report No. CEER/R92-08*, 2003.

Weng,Y.T. (2003) "A Study of Multi-mode Seismic Performance-based Evaluation and Displacement-based Design Procedures", Ph.D. Thesis, Supervised by Prof. Keh-Chyuan Tsai, Department of Civil Engineering, National Taiwan University, Taipei, Taiwan, in preparation, to be available in July, 2003.

Yang, Y.S., Wang, S.J., Wang, K.J., Tsai, K.C. and Hsieh, S.H., "ISEE: Internet-Based Simulations for Earthquake Engineering Part I: The Database Approach", Proceedings, International workshop on Steel and Concrete Composite Constructions, Taipei, Oct. 2003.

Table 1. Proposed building performance levels for the CFT/BRB frame specimen

	Building Performance
Life Safefy (10/50-0.02 hazard/performance)	Many buckling restrained braces yield. Beam-to-column moment connection should not fail.
	Transient inter-story drift limit=0.02 radian Permanent inter-story drift limit=0.005 radian
Collapse Prevention (2/50-0.025 hazard/performance)	Extensive yielding of braces. Braces and its connections should not fail. Some beam-to-column moment connections may fail.
	Transient inter-story Drift limit=0.025 radian Permanent inter-story Drift limit=0.01 radian

Table 2. Material test results

		Positions of Sampling		f_y (MPa)	f_u (MPa)
Steel (A572Gr.50)	3FL	Beam	Flange	372	468
			Web	426	493
		BRB3	core steel material	373	483
	2FL	Beam	Flange	414	503
			Web	482	538
		BRB2	core steel material	397	545
	1FL	Beam	Flange	370	486
			Web	354	485
		BRB1	core steel material	421	534
C1(Tube-400-9)		Steel		374, 488	488
		Concrete		f_c'=35 MPa	
C2(Pipe-400-9)		Steel		543	584
		Concrete		f_c'=35 MPa	

Table 3. Computation of story ductility and system ductility

(a)All steel material strength are nominal

Story	α_{ci}	Story Ductility					
		10/50			2/50		
		θ_{yi}	θ_{mi}	μ_i	θ_{yi}	θ_{mi}	μ_i
		unit : 1/1000 rad			unit : 1/1000 rad		
3F	0.50	1.74	20	9.19	1.74	25	11.5
2F	0.50	1.74	20	9.19	1.74	25	11.5
1F	0.50	1.74	20	9.19	1.74	25	11.5
Average		1.74	20	9.19	1.74	25	11.5

(b) All steel material strength are based on tensile coupon test results

Story	α_{ci}	Story Ductility					
		10/50			2/50		
		θ_{yi}	θ_{mi}	μ_i	θ_{yi}	θ_{mi}	μ_i
		unit : 1/1000 rad			unit : 1/1000 rad		
3F	0.57	2.42	20	6.61	2.42	25	8.27
2F	0.49	1.96	20	8.15	1.96	25	10.2
1F	0.60	2.26	20	7.08	2.26	25	8.85
Average		2.21	20	7.28	2.21	25	9.10

Table 4. Comparison of design lateral story forces and elastic period

Story	Lateral Story Force (kN)			
	Frame 10/50-Tri	Frame 10/50-TriMR	Frame 2/50-Tri	Frame 2/50-TriMR
3F	620.6	693.4	786.2	889.8
2F	526.2	587.9	666.5	754.3
1F	263.1	293.9	333.3	377.2
Sum	1409.9	1575.2	1786.0	2021.3
Elastic Period (sec)	0.70	0.72	0.68	0.70

Table 5. Comparison of member sizes of CFT/BRB frame specimen

Frame Label	Core Cross Sectional Area of Braces (A572 GR50) unit : cm^2		
	1FL (BRB1)	2FL (BRB2)	3FL (BRB3)
2/50-Tri	34	27	15
2/50-TriMR	30	25	15
Dimension of Columns (A572 GR50) unit : mm		C1: Tube: 350×9, C2: Pipe: 400×9	
Dimension of Beams (A572 GR50) unit : mm			
3FL	3B1~3B3:H400×200×8×13		
2FL	2B1~2B3:H450×200×9×14		
1FL	1B1~1B3:H456×201×10×17		

Table 6. The ratio of inelastic axial cumulative deformation (Δ_{inel}) to tensile yield displacement (Δ_y) of BRB members obtained in dynamic time history analyses

	Δ_{inel}/Δ_y			
Floor	50/50	10/50	2/50	End
3FL	23.7	133	345	455
2FL	29.8	121	313	402
1FL	6.47	34.4	127	152

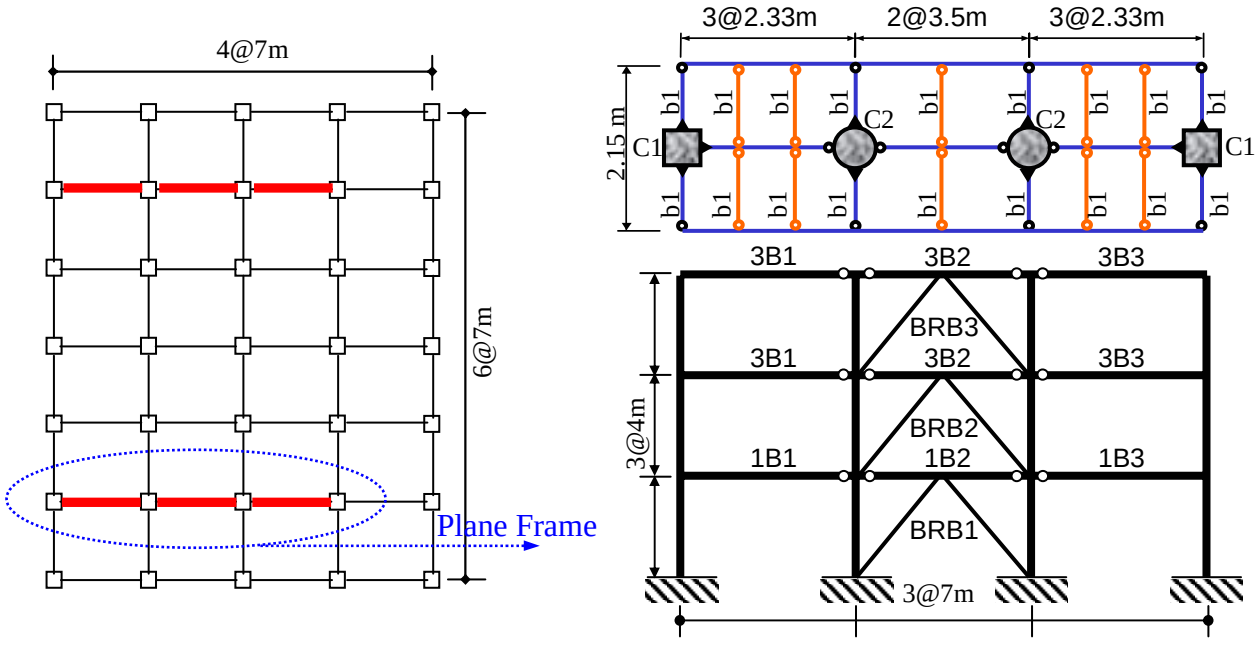

Fig.1 Floor framing plan and elevation

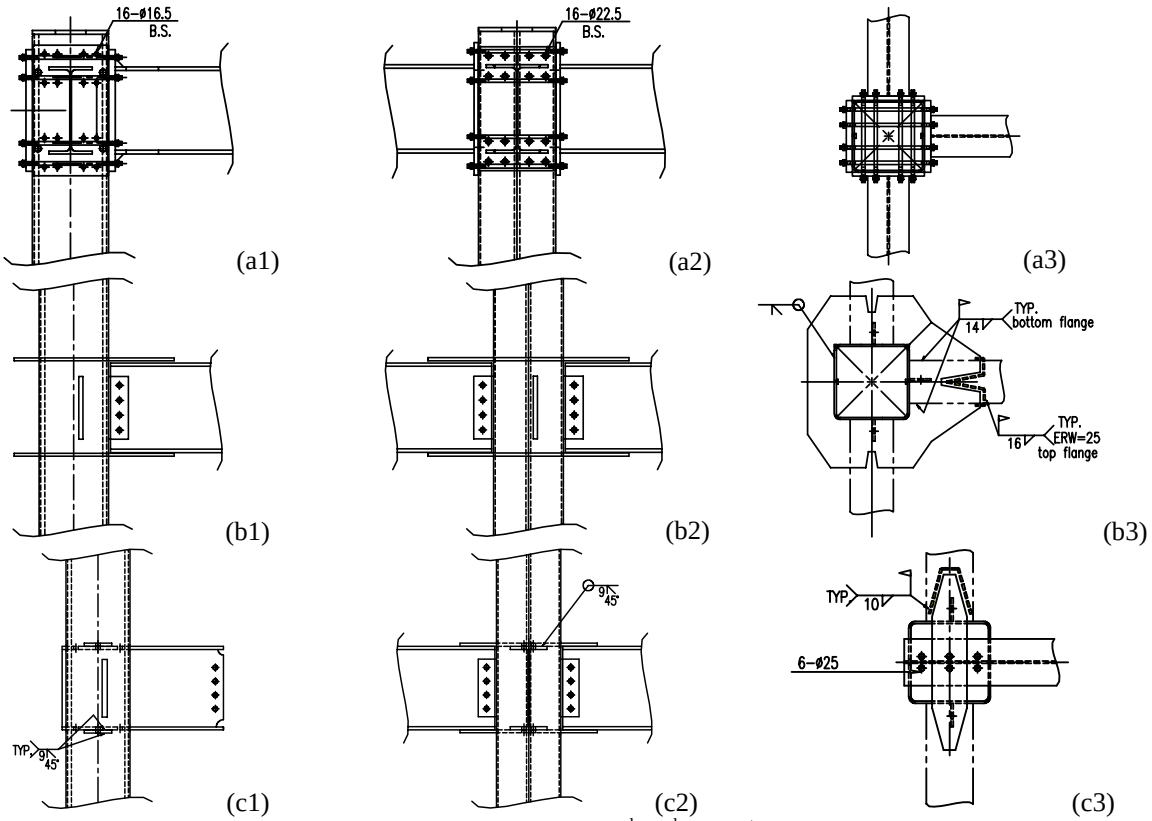

Fig.2 Moment connection details (a, b, c for 3rd, 2nd and 1st floor, respectively)

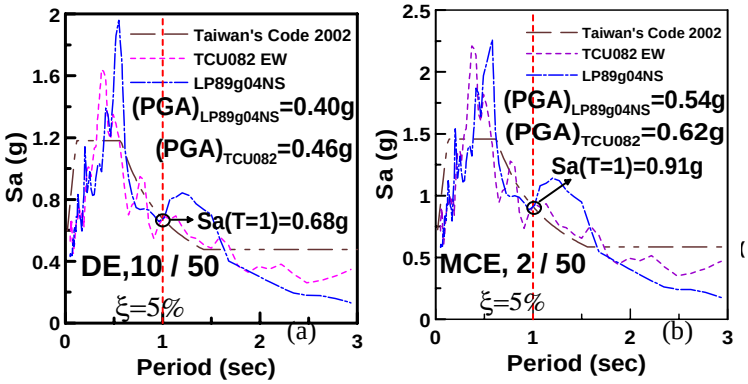

Fig. 3 Design acceleration spectra (a)10/50 (b)2/50 hazard level

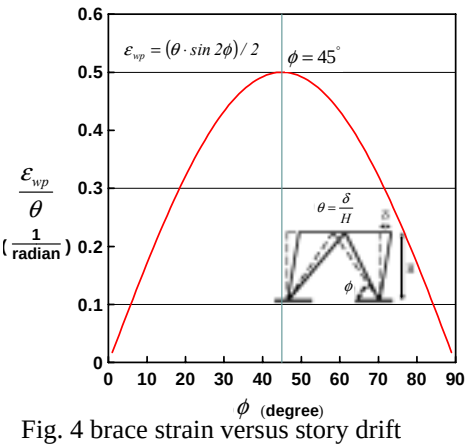

Fig. 4 brace strain versus story drift relationships

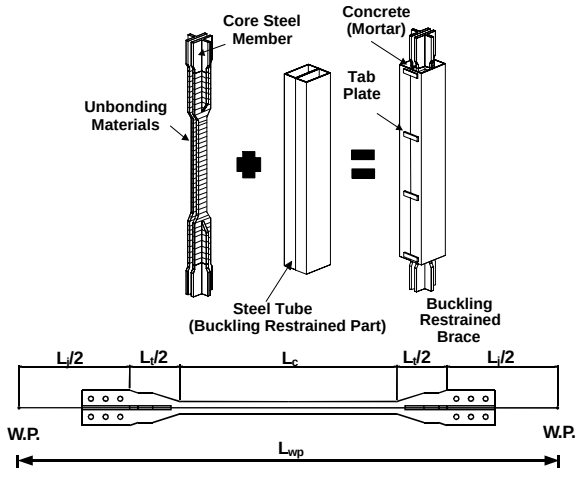

Fig. 5 Profiles of core steel in the BRB

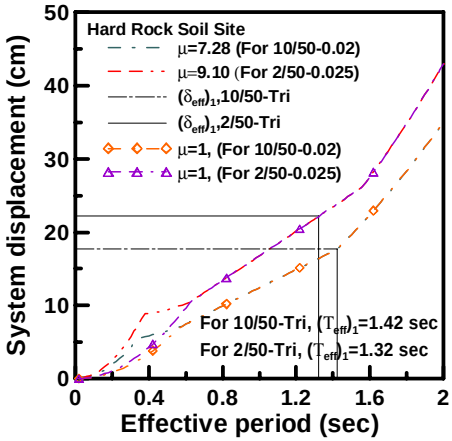

Fig.6 Inelastic Design Displacement Spectra

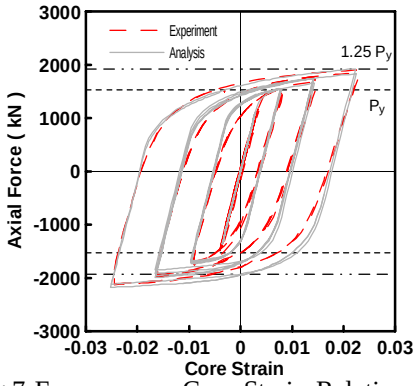

Fig.7 Force versus Core Strain Relationship of BRB using A572 Gr.50

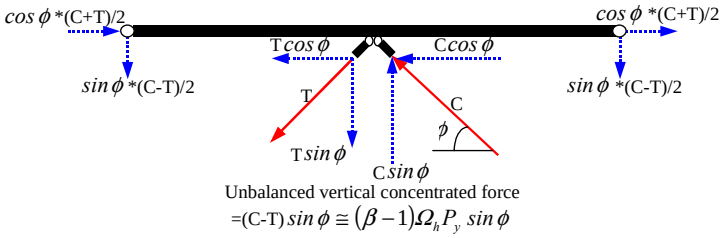

Fig.8 Free Body Diagram of a Beam Supporting the BRBs

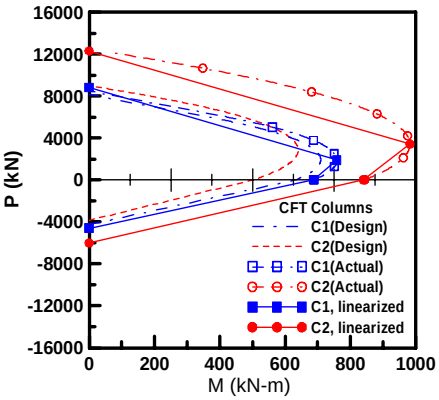

Fig. 11 P-M interactive curves of CFT columns

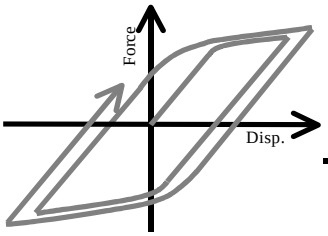

Fig. 9 Two-surface plasticity hardening truss element

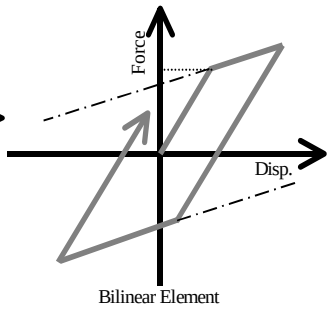

Fig. 10 Bilinear element model

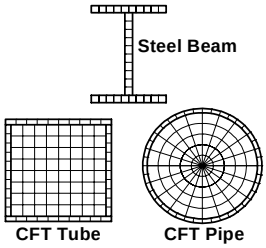

Fig. 12 Fiber sections in OpenSees

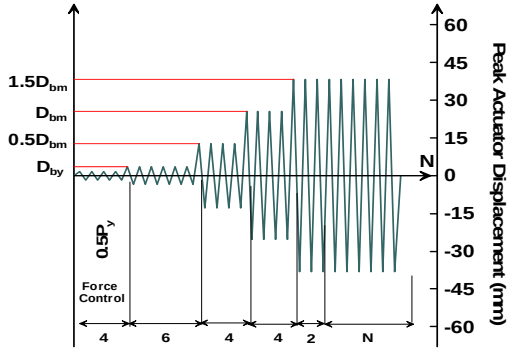

Fig.13 Cyclic axial displacement history for two-surface plasticity brace element (core length=1700mm)

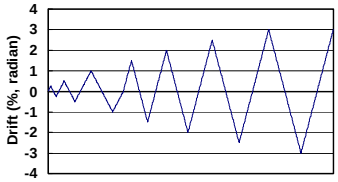

Fig.14 Lateral cyclic drift history for the beam-column element

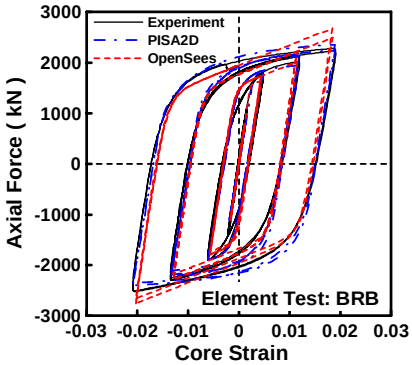

Fig. 15 BRB element models

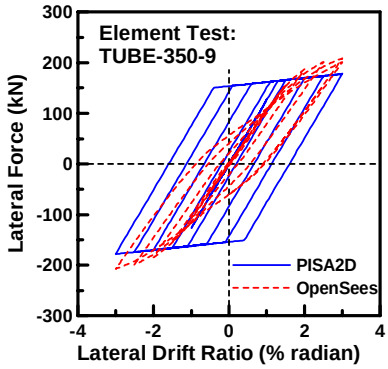

Fig. 16 CFT models (Tube 350-9)

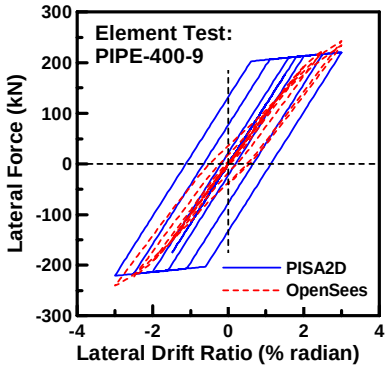

Fig. 17 CFT models (Pipe 400-9)

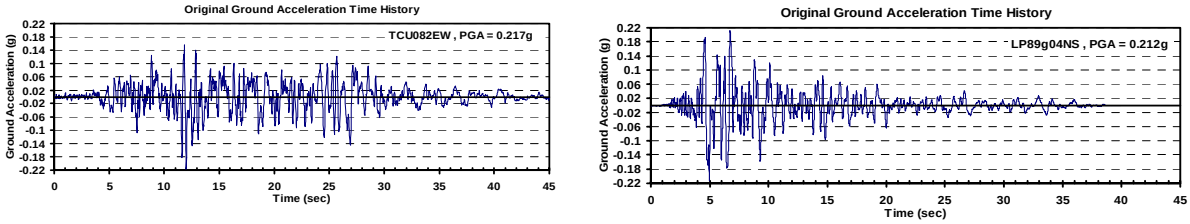

Fig. 18 Original ground accelerations used in test (before scaling)

50/50 event → 10/50 event → 2/50 event → 10/50 event

⇩ ⇩ ⇩ ⇩

TCU082 EW → LP89g04 NS → TCU082 EW → LP89g04 NS

Fig. 19 Earthquake sequence applied in this study

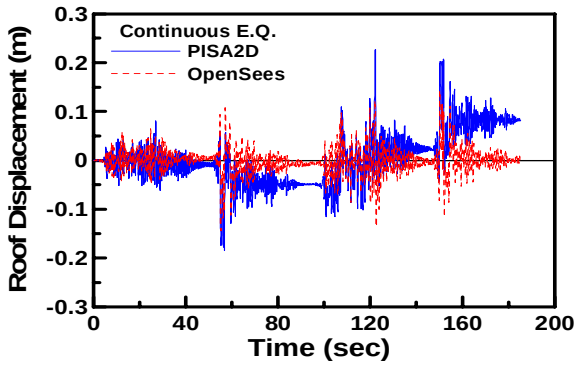

Fig. 20 Analytical roof displacement time history

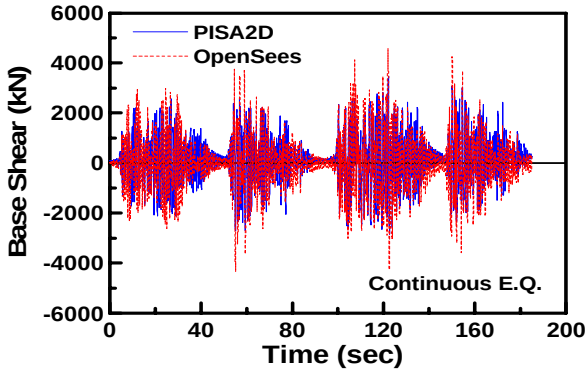

Fig. 21 Analytical base shear time history

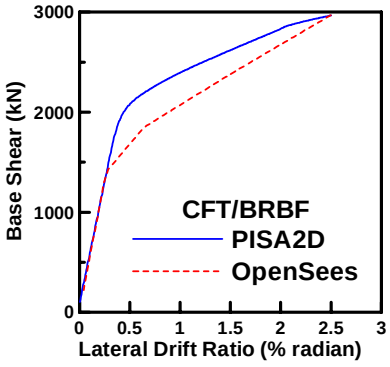

Fig. 22 Results of pushover analysis for Frame 2/50-TriMR

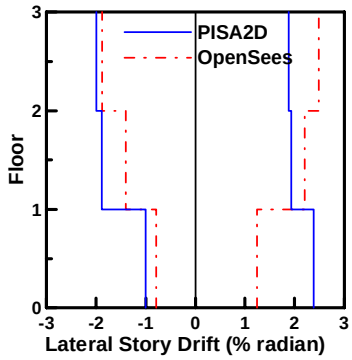

Fig. 23 Story drift distribution of Frame 2/50-TriMR

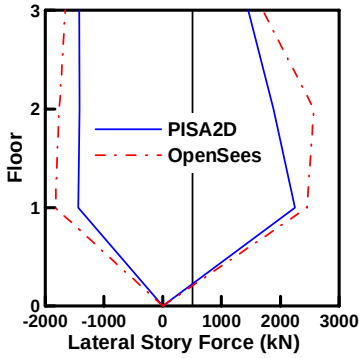

Fig. 24 Lateral story force distribution of Frame 2/50-TriMR

Fig. 25 Plastic hinge distributions obtained from VISA2D program